A Planar Gyroscope Using a Standard Surface Micromachining Process

S. E. Alper[1] and T. Akin[1,2]
[1]Middle East Technical University, Dept. of Electrical and Electronics Eng., 06531 Ankara, Turkey
[2] TUBITAK-ODTU-BILTEN, Middle East Technical University, 06531 Ankara, Turkey
e-mail: tayfun-akin@metu.edu.tr http://www.eee.metu.edu.tr/~tayfuna

Summary. *This paper presents a planar gyroscope based on a standard three-layer polysilicon surface micromachining process. Structural geometry is designed to minimize the effects of limitations coming from the standard surface micromachining. Finite element simulations are carried out, and mismatches of resonant frequencies of the drive and sense mode vibrations are reduced down to 0.5% in order to achieve increased performance. The third polysilicon layer on top of outer gimbal is used for feedback control and for tuning of the resonant frequency. The drive and sense capacitance values are 2.48 pF and 0.58 pF, respectively. The device measures about 900µmx550µm area with a 2µm thick structural layer. The fabricated structures are tested and their resonant frequencies are measured as 5119 Hz and 4889 Hz for the drive and sense vibration modes, respectively. The frequency mismatch is 4.65% for these two modes and the resonant frequencies can be adjusted by varying the dc bias voltage applied to the proof mass. A capacitive readout circuit was developed in a 0. 8 µm CMOS process to be hybrid connected to the gyroscope. The fabricated readout circuit can detect capacitance changes smaller than 0.1fF and provide a sensitivity of 45mV/fF.*

Keywords: micromachined gyroscopes, resonant frequency tuning, finite element simulations

Introduction

Micromachined gyroscopes have found large attention in recent years due to their low cost and small size, and there are extensive studies with different approaches to implement gyroscopes with increased performance and high yield for industrial use [1]. Some approaches use non-standard fabrication techniques and obtain high performance devices [2], but commercialization of such devices is expected to take time. A different approach is to use standard micromachining processes offered by industrial foundries, such as the three-layer polysilicon surface micromachining process provided by MCNC-CRONOS. However, these processes limit the gyroscope structures and performances. For example, structural layer thickness is limited with 2µm for a standard polysilicon process, resulting in small capacitance value for comb finger type drive and sense mechanisms. Another problem is the buckling of the large dimension devices, which may result in the level shifting between stationary and proof mass fingers, substantially reducing the already small capacitance between them [3].

This paper describes a planar gyroscope that overcomes the small layer thickness and buckling problems in standard polysilicon surface micromachined foundry processes. The structure provides large drive and sense capacitance values allowing the structure to be excited with practical voltage levels and increasing its sensitivity to angular rate. In addition, it allows to electrostatically control the resonant frequencies of the drive and sense modes.

Gyroscope structure and operation

Figure 1 shows the structure of the planar gyroscope implemented in a standard polysilicon surface micromachining process. The structure is composed of an outer gimbal fixed to the substrate via anchors, an inner gimbal connected to the outer gimbal through torsional support flexures, drive/control electrodes below and above the outer gimbal, and sense electrodes under the inner gimbal.

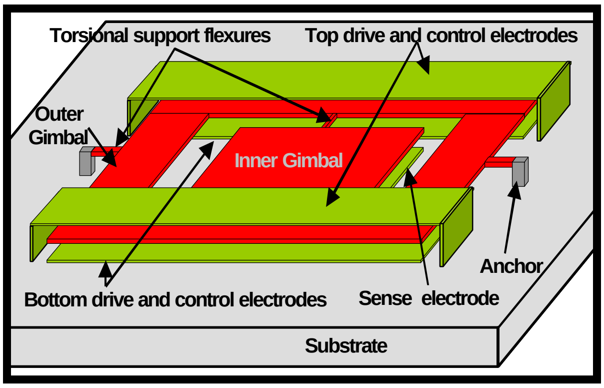

Fig. 1: Structural view of the planar micromachined gyroscope.

Operation of the planar gyroscope depends on Coriolis coupling effect. When the outer gimbal is excited to vibrate torsionally and an input rotation rate is applied around an axis vertical to the substrate, the inner gimbal starts vibrating torsionally. By sensing the motion of the inner gimbal with a capacitive readout circuit, the rotation information is obtained. There are two isolated electrodes under the

ISBN 87-89935-50-0

inner gimbal, allowing to use differential sensing scheme. Excitation of the outer gimbal can be achieved with both the top and bottom drive electrodes. Having two electrodes allows more efficient electrostatic feedback control and better adjustment of resonant frequency of the drive vibration mode.

This planar gyroscope structure has a number of advantages compared with polysilicon comb drive gyroscopes. First of all, the device has large drive and sense capacitance values, because, for both of the vibration modes, the capacitance is between the proof mass and substrate electrode placed underneath the mass. The second advantage is that small bucklings do not cause vital problem in the device operation, since buckling occurs along an axis vertical to the substrate; there is no possibility that the capacitance plates are misaligned. The third advantage is the enhanced sensitivity due to possible large drive amplitudes. Finally, the resonant frequencies of the two vibration modes can be both increased and decreased by the sandwich-like drive electrodes and sense electrodes, by adjusting the gap between the proof mass and substrate. This also allows matching of the resonant frequencies of the drive and sense modes electrostatically using DC bias voltages.

Optimization and simulations

FEM simulations were used for optimizing the dimensions of the sensor in order to match the resonant frequencies of the drive and sense modes. Matching of the resonant frequencies improves the performance by causing the sensitivity to be amplified by the mechanical quality factor of the sense resonance mode of the structure [4]. Simulations for adjusting the resonant frequencies of the drive and sense vibration modes were performed using ANSYS 5.4 software. Figure 2 and 3 shows the results of the simulations, which demonstrate the drive and sense mode resonant frequencies as 5337 Hz and 5312 Hz, respectively. Clearly, frequency mismatch between the two vibration modes is smaller than 0.5%.

Table 1: Summary of the device parameters of the planar gyroscope. The device occupies a large area for a surface micromachined sensor and also has quite large capacitance values.

Parameter	Value
Outer length	920 μm
Outer width	540 μm
Structural thickness	2 μm
Capacitive gap	2 μm
Drive capacitance	1.24 pF x 2
Sense capacitance	0.29 pF x 2

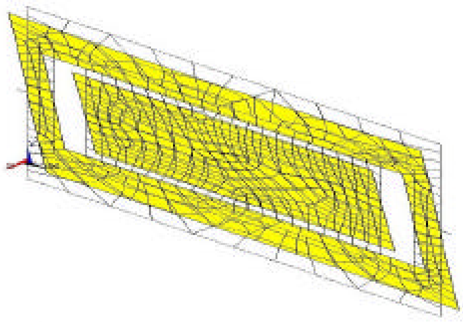

Fig. 2: FEM result of the drive mode vibrations. Resonant frequency of this mode is determined as 5337 Hz.

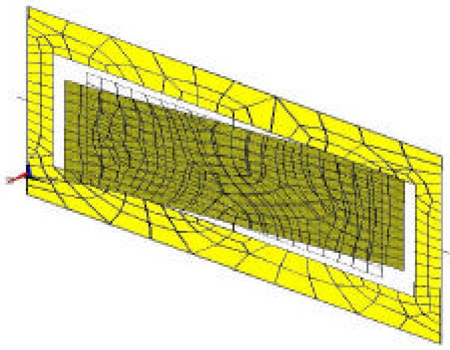

Fig. 3: FEM result of the sense mode vibrations. Resonant frequency is 5312 Hz, very close to the drive mode frequency.

Implementation and test results

The planar gyroscope structure has been implemented through three polysilicon surface micromachining process provided by MCNC-CRONOS. Figure 4 shows the SEM picture of the fabricated planar gyroscope, and Table 1 summarizes its device parameters, including dimensions and capacitance values. Operation of the device is verified by electrostatically actuating the fabricated structures, and no stiction is observed despite large device dimensions.

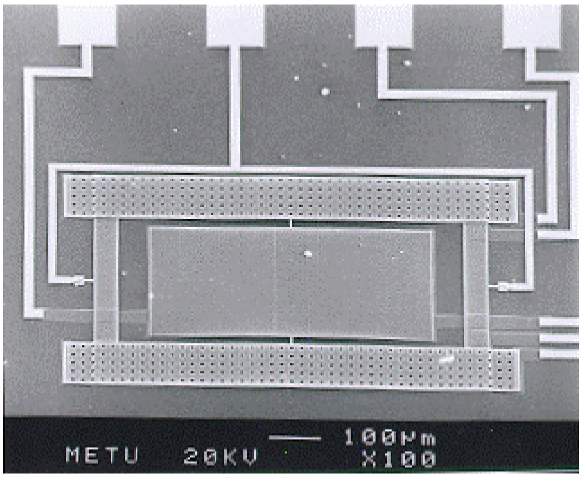

Fig. 4: SEM view of the fabricated planar gyroscope. The device measures 920μmx540μm.

A number of tests performed to verify the device operation and to characterize the performance and resonant frequencies. Resonant frequencies of the drive and sense vibration modes of the planar gyroscope were measured by HP4395A Network/Spectrum Analyzer. These measurements were performed by using a unity gain buffer circuit chip which was hybrid connected to the sensor. The buffer chip allows to monitor the high impedance output signal from the gyroscope. Figure 5 shows resonant frequency measurement results for (a) drive and (b) sense modes. Drive and sense mode resonant frequencies were measured as 5119.5 Hz and 4889 Hz, respectively, when a 0.5V DC polarization voltage applied to the proof mass. The measured results show small differences from the simulated values. The differences arise from lithographical steps in the fabrication and the internal stress of the polysilicon which was not included in simulations. There is also a mismatch of approximately 4.65% between the measured values of the drive and sense resonant frequencies. Table 2 shows the simulated and measured frequencies and the mismatch value. The mismach in the resonant frequencies can be reduced by applying different DC bias voltages to the sense and drive electrodes seperately.

Figure 6 shows the change in resonant frequencies of the drive and sense modes with DC bias voltages. Changing the dc bias voltage by only few hundreds of millivolts, the resonant frequencies can be adjusted in ranges of 150Hz for the drive mode and 250 Hz for the sense mode, thanks to large capacitances obtained by the planar structure. By applying 0.5V between the sense electrode and the proof mass and 1V between the drive electrode and the proof mass, the resonant frequency mismatch can be decreased to 1.8%. Applying a lower voltage than 0.5V to the sense electrode is not suggested, since it decrases linearity of the sensor output. Similarly, applying a higher voltage than 1V to the drive electrode is not suggested, since since above that value the edges of outer and inner gimbals touch to the drive electrodes, respectively. The reason for this is the buckled edges of the gimbals. Although buckling is not a vital problem for this gyroscope structure, it causes the edges of the large plates to be bent, limiting the DC voltage control. This is a bigger problem for the top drive and control electrodes in this technology, since the thickness between the top electrodes and the proff mass is only 0.8 µm (the thickness between the bottom electrode and proof mass is 2µm). These problems can be solved by designing the top and bottom electrodes smaller in such a way that, edges of the gimbals can never touch these electrodes.

The operation voltages mentioned are very low compared to comb drive gyroscopes, since the planar gyroscope have much larger capacitances. These large capacitances also allows to exite the sensor with very small AC drive voltages of about 60mV-peak, even though the sensor has a big proof mass.

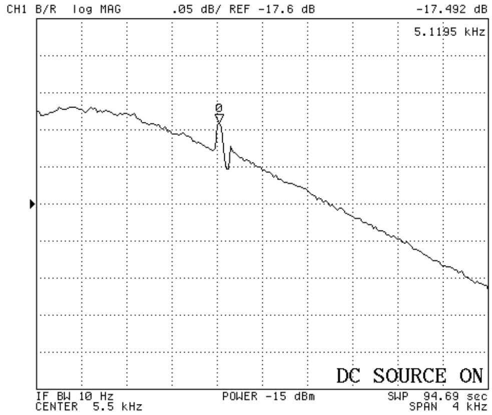

(a)

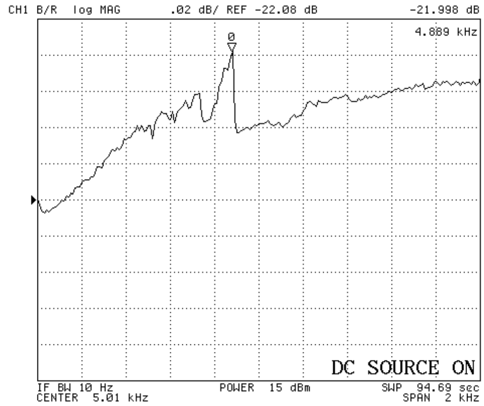

(b)

Fig. 5: Resonant frequency measurement results for (a) drive and (b) sense modes. Drive and sense mode resonant frequencies were measured as 5119.5 Hz and 4889 Hz, respectively, when a 0.5V DC polarization voltage applied to the proof mass.

Table 2: Comparison of the simulated and measured resonant frequency data.

Parameter	Simulated	Measured (for 0.5V DC bias)
Drive resonant frequency (Hz)	5337	5119.5
Sense resonant frequency (Hz)	5312	4889
Mismatch (%)	0.47	4.65

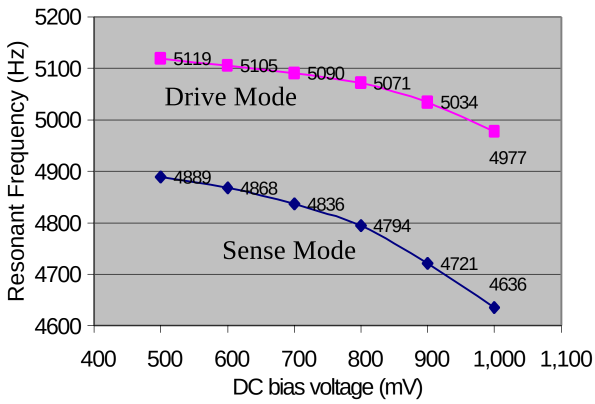

Fig. 6: Resonant frequency versus DC bias voltage for the drive and sense modes of the gyroscope.

Readout Electronics

Readout electronics is necessary to obtain a voltage output as response to rotation. The gyroscope is designed to provide a differential capacitance change, so that a very sensitive readout circuit can be implemented. Figure 7 show the block diagram of the differential capacitive readout circuit. The circuit senses the difference between the capacitors $C_{sensor+}$ and $C_{sensor-}$ and shifts the voltage at the common node of the capacitors. This shift is integrated by the integrator which is then fed to the correlated double sampling (CDS) circuit. The CDS block is used for cancelling possible shifts which may arise due to op amp offsets and switch noises. The CDS output is connected to the comparator, whose output is a one-bit digital signal. For closed loop operation this signal may be processed by a latch, and the latch output can be fed back to the commmon node of the capacitors cancelling the sensor capacitance deflection.

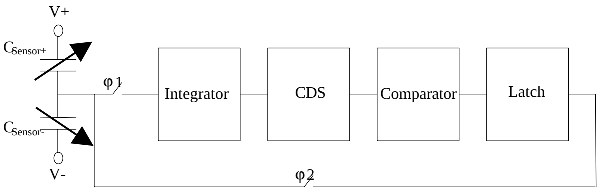

Fig. 7: Block diagram of the capacitive readout circuit. Non-overlapping clocks φ1 and φ2 are for processing and for feedback, respectively.

Figure 8 shows a photograph of the capacitive readout circuit that was fabricated using a 0.8µm CMOS process. The circuit occupies a 700µmx550µm area. Initial tests show that the circuit is operational and it provides a sensitivity close to its design value. Figure 9 shows the output of the readout circuit when $C_{sensor+}$ is approximately 40 fF larger than $C_{sensor-}$. The output voltage shifts about 1.8V, showing that the circuit provides a sensitivity of 45mV/fF and detects a capacitance difference lower than 0.1fF.

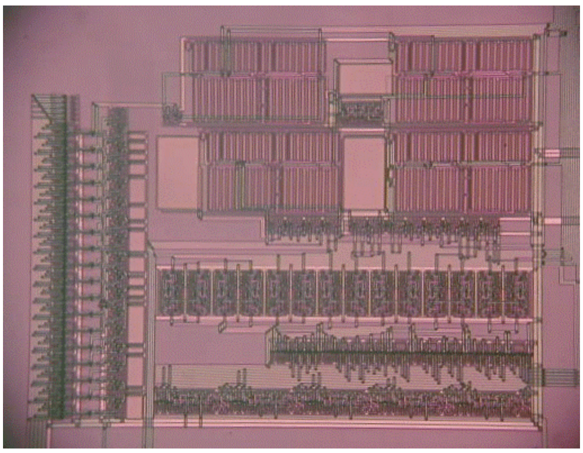

Fig. 8: Photograph of the capacitive readout circuit fabricated in a 0.8 µm CMOS process. The circuit occupies a 700µmx550µm area.

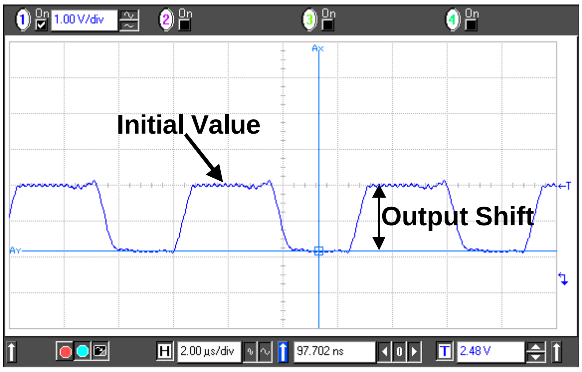

Fig. 9: The output of the readout circuit when $C_{sensor+}$ is approximately 40 fF larger than $C_{sensor-}$. The output voltage shifts about 1.8V, showing that the circuit provides a sensitivity of 45mV/fF and detects a capacitance difference lower than 0.1fF.

Conclusions and Future Work

A planar gyroscope based on a standard three-layer polysilicon process is presented. Contrary to conventional comb-drive gyroscopes, this device have large capacitance values in the order of picofarads owing to its structural geometry.

The device structure was optimized to have matched resonant frequencies for the drive and sense vibration modes using FEM modeling and simulations. Measured resonant frequencies of the fabricated devices are close to the design values, but there are small differences due to process variations. Resonant frequencies of the drive and sense modes of the gyroscope can be shifted by more than 3%, by changing the DC bias voltage from 0.5V to 1V. Bias voltages higher than 1.5 V cause the buckled edges of the gimbals touch to the drive electrodes, creating a problem in device operation.

A capacitive read-out circuit was designed and fabricated which will be hybrid connected to the sensor to measure the sense vibrations arising from the angular rates. Initial tests show that the circuit provides a sensitivity of 45mV/fF and detects a capacitance difference lower than 0.1fF. This circuit will be connected to the planar gyroscope to measure its rate sensitivity.

References

[1] N. Yazdi, F. Ayazi, and K. Najafi. "Micromachined Inertial Sensors," *Proc. of the IEEE,* vol. 86, no. 8 (1998) 1640-1659.

[2] F. Ayazi and K. Najafi. "Design and Fabrication of a High-Performance Polysilicon Vibrating Ring Gyroscope," *IEEE Micro Electro Mechanical System Workshop (MEMS98)* , pp. 621-626, February 1998.

[3] W. C. Tang, T. H. Nguyen, and R. T. Howe. "Laterally Driven Polysilicon Resonant Microstructures," *Sensors and Actuators A,* 20 (1989) 25-32.

[4] P. Greiff, B. Boxenhorn, T. King, and L. Niles. Silicon Monolithic Micromechanical Gyroscope," *Int. Conf. Solid-State Sensors and Actuators (TRANSDUCERS91),* pp. 966-968, June 1991.